Available online at www.sciencedirect.com
SCIENCE DIRECT®
Archives of Biochemistry and Biophysics 437 (2005) 106–114
ABB
www.elsevier.com/locate/yabbi

Proton transfer from exogenous donors in catalysis by human carbonic anhydrase II

Ileana Elder [a], Chingkuang Tu [a], Li-June Ming [b], Robert McKenna [c], David N. Silverman [a,*]

[a] Department of Pharmacology and Therapeutics, University of Florida College of Medicine, Gainesville, FL 32610-0267, USA
[b] Department of Chemistry and Institute for Biomolecular Science, University of South Florida, 4202 Fowler Avenue, Tampa, FL 33620-5250, USA
[c] Department of Biochemistry and Molecular Biology, University of Florida College of Medicine, Gainesville, FL 32610-0267, USA

Received 9 February 2005, and in revised form 9 February 2005
Available online 17 March 2005

Abstract

In the site-specific mutant of human carbonic anhydrase in which the proton shuttle His64 is replaced with alanine, H64A HCA II, catalysis can be activated in a saturable manner by the proton donor 4-methylimidazole (4-MI). From ^{1}H NMR relaxivities, we found 4-MI bound as a second-shell ligand of the tetrahedrally coordinated cobalt in Co(II)-substituted H64A HCA II, with 4-MI located about 4.5 Å from the metal. Binding constants of 4-MI to H64A HCA II were estimated from: (1) NMR relaxation of the protons of 4-MI by Co(II)-H64A HCA II, (2) the visible absorption spectrum of Co(II)-H64A HCA II in the presence of 4-MI, (3) the inhibition by 4-MI of the catalytic hydration of CO_2, and (4) from the catalyzed exchange of ^{18}O between CO_2 and water. These experiments along with previously reported crystallographic and catalytic data help identify a range of distances at which proton transfer is efficient in carbonic anhydrase II.
© 2005 Elsevier Inc. All rights reserved.

Keywords: Proton transfer; Magnetic resonance; Carbon dioxide; Carbonic anhydrase; Isotope exchange; Enzyme activation

Carbonic anhydrase II, one of the most efficient isozymes in the α class of carbonic anhydrases [1,2], catalyzes the hydration of CO_2 in two stages [2,3]. The first is the conversion of CO_2 into bicarbonate by reaction with a zinc-bound hydroxide; the dissociation of bicarbonate leaves a water molecule at the zinc (Eq. (1))

$$CO_2 + EZnOH^- \rightleftharpoons EZnHCO_3^- \overset{[H_2O]}{\rightleftharpoons} EZnH_2O + HCO_3^-. \quad (1)$$

The second step is the transfer of a proton to regenerate the zinc-bound hydroxide (Eq. (2)); here B denotes a proton acceptor, either an exogenous proton acceptor from solution or a residue of the enzyme itself.

$$EZnH_2O + B \rightleftharpoons EZnOH^- + BH^+. \quad (2)$$

A number of studies have shown that His64 in human carbonic anhydrase II (HCA II)[1] functions as a proton acceptor/donor in the shuttling pathway [2–5]; that is, His64 acts as the proton transfer residue B of Eq. (2). The three-dimensional structure of wild-type HCA II at pH 8.5 shows His64 located in the active-site cavity with its imidazole ring approximately 7.5 Å from the zinc ion when this side chain

* Corresponding author. Fax: +1 352 392 9696.
E-mail address: silvermn@college.med.ufl.edu (D.N. Silverman).

[1] *Abbreviations used:* HCA II, human carbonic anhydrase II; H64A HCA II, the mutant of human carbonic anhydrase II with His64 replaced with Ala; 4-MI, 4-methylimidazole; Co(II)-H64A HCA II, cobalt-substituted H64A HCA II; TSP-d_4, sodium 3-trimethylsilyl-2,2,3,3-tetradeuteropropionate; Hepes, *N*-(2-hydroxyethyl)piperazine-*N*′-(2-ethanesulfonic acid).

0003-9861/$ - see front matter © 2005 Elsevier Inc. All rights reserved.
doi:10.1016/j.abb.2005.03.001

is the "in" conformation oriented roughly in the direction of the zinc [6–8]. The position of His64 and its distance from the zinc ion suggest that proton transfer proceeds through intervening hydrogen-bonded water bridges.

A decrease in catalysis by a site-specific mutant of HCA II in which His64 is replaced by Ala (H64A HCA II) supports the hypothesis that His64 participates in the proton transport pathway [5]. The turnover number for catalysis, k_{cat}, of CO_2 hydration by H64A HCA II was decreased approximately 10- to 100-fold compared to the wild-type enzyme. The decrease in catalysis could be rescued in a saturable manner by the addition of exogenous proton acceptors in solution, such as imidazole, pyridine, and derivatives [5,9]. It has been an intriguing observation that the chemical rescue of H64A HCA II by small exogenous proton donors and acceptors is substantial, with catalysis at saturation levels of certain imidazole and pyridine derivatives approaching that of wild-type HCA II [10]. This suggests that useful information about proton translocation in carbonic anhydrase could be obtained by kinetic analysis of the extent of activation of H64A HCA II by exogenous proton acceptors and donors, and by structural localization of the binding sites of these exogenous agents.

Although binding sites within the active-site cavity have been estimated by X-ray crystallography for activators and small molecules [9–11], it is not clear that these represent sites from which proton transfer occurs. For example, X-ray diffraction of H64A HCA II crystals soaked in 4-methylimidazole (4-MI) showed a binding site 12 Å from the zinc ion associated with Trp5 in the active-site cavity [10]; however, this binding site was not productive in proton transfer in catalysis as demonstrated with subsequent kinetic analysis [9]. Moreover, imidazole and other heterocyclic aromatic compounds can be inhibitors of carbonic anhydrase by binding at or near the metal [2].

To observe the effect of these exogenous proton donors on catalysis by H64A HCA II, we have made kinetic and structural measurements to establish the range of distances for efficient proton transfer. 4-MI binds in the active-site cavity of H64A HCA II at three known locations with distances from 4.5 to 13 Å from the metal. Although 4-MI is an activator of carbonic anhydrase through a proton transfer mechanism, data show that none of these sites are productive in proton transfer. Comparison of catalytic and structural data on other known proton donors in this catalysis shows that the binding sites of 4-MI that we have located help establish distances that are upper and lower limits for proton transfer in the active site of HCA II. These features are discussed in terms of the requirements for proton transfer in an active-site environment.

Materials and methods

Enzymes

Site-specific mutants of HCA II (H64A; H64A-E69A-D72A) were prepared and expressed by transforming into *Escherichia coli* BL21(DE3)pLysS [12] as previously described [5,9]. The sequences were confirmed from the DNA of the entire coding region for carbonic anhydrase in the expression vector. Carbonic anhydrases were purified using affinity chromatography with *p*-(aminomethyl)-benzenesulfonamide coupled to agarose beads [13], followed by extensive dialysis. Matrix assisted laser desorption ionization–time-of-flight mass spectrometry gave results consistent with the protein sequences. Purity of enzyme samples was verified by electrophoresis on a 10% polyacrylamide gel stained with Coomassie. Concentrations of HCA II and mutants were determined from the molar absorptivity at 280 nm ($5.5 \times 10^4\ M^{-1}\ cm^{-1}$) and by titration with the tight binding inhibitor ethoxzolamide while observing enzyme catalyzed ^{18}O exchange between CO_2 and water. These two methods gave excellent agreement.

Metal substitution

Apo-H64A HCA II was made by addition of 0.5 M dipicolinic acid to enzyme in 0.25 M Hepes buffer at pH 7.3 and stirring for 4 h at 4 °C. After extensive dialysis against 1 mM Tris at pH 8.0 under N_2 to remove chelator from solution, $CoSO_4$ (final concentration 1 mM) was added. Excess cobalt was removed by dialysis against 1 mM Tris, pH 8.0. Metal substitution was verified from the visible absorption spectrum; Co(II)-substituted HCA II has two distinctive maximal absorbances at 618 and 640 nm [14]. The concentration of Co(II)-H64A HCA II was determined by titration with ethoxzolamide while observing catalytic ^{18}O exchange.

^1H NMR of the complex of 4-MI and H64A HCA II

Samples (0.6 ml) containing 0.5 mM Co(II)-H64A HCA II in 1 mM Tris and 8 mM of TSP-d_4 reference standard in 60% D_2O were placed in 5 mm NMR tubes. ^1H NMR spectra were obtained at 25 °C on a Bruker Avance spectrometer at 500 MHz. Typical spectra consisted of 8–16 scans with 16 K data points over a spectral width of 12 kHz. An additional 5 Hz line broadening was introduced to all spectra to improve signal-to-noise ratio. Spectra for the diamagnetic sample Zn(II)-H64A HCA II were measured under the same conditions as for the Co(II)-substituted enzyme. Proton spin–lattice relaxation times, T_1, were measured by the inversion–recovery method (180 °–τ–90 °) after estimation of the longest T_1 for 4-MI protons. A total of 10 variable delay time values were used for each run.

The inversion–recovery pulse sequence included a presaturation of 54 dB for suppression of the water signal.

The paramagnetic contribution to the proton relaxation rate of 4-MI, T_{1P}^{-1}, was obtained by subtracting the relaxation rate of 4-MI in the presence of Zn(II)-H64A HCA II from the relaxation rate in the presence of Co(II)-H64A HCA II. The normalized relaxation rate, $T_{1P}^{-1}/[E]$, as a function of 4-MI concentration was fitted with Eq. (3) [15–17] for a single 4-MI binding site on Co(II)-H64A HCA II to obtain T_{1M}^{-1}, the relaxation rate of bound 4-MI. In Eq. (3), K_D is the equilibrium dissociation constant for 4-MI binding, $T_{1P}^{-1}/[E]$ is the relaxivity, and [E] is the total concentration of Co(II)-H64A HCA II (0.5 mM)

$$T_{1P}^{-1}/[E] = T_{1M}^{-1}/(K_D + [4\text{-MI}]). \quad (3)$$

The Solomon equation (Eq. (4)) was used to analyze T_{1M}^{-1} for proton resonances of the 4-MI bound to the paramagnetic enzyme and to calculate averaged distances between 4-MI binding sites and the paramagnetic cobalt, assuming a predominant dipolar contribution to the relaxation [18,19]. In this equation, μ_0 is the permeability of vacuum, γ_N is the magnetogyric ratio, g_e is the electron g factor, μ_B is the electron Bohr magneton, S is the total electron spin, τ_c is a correlation time, ω_I and ω_S are the nuclear and electron Larmor precession frequencies, and r is the distance between the monitored ^{1}H nuclei and the paramagnetic cobalt

$$T_{1M}^{-1} = \frac{2}{15}\left(\frac{\mu_o}{4\pi}\right)^2 \times \frac{\gamma_N^2 g_e^2 \mu_B^2 S(S+1)}{r^6}\left[\frac{7\tau_c}{1+\omega_s^2\tau_c^2} + \frac{3\tau_c}{1+\omega_I^2\tau_c^2}\right]. \quad (4)$$

The correlation time τ_c used for our calculations is dominated by the electronic relaxation time (10^{-11}–5×10^{-13} s) characteristic of four- and five-coordinated Co(II)-substituted CA [15,20–22].

Oxygen-18 exchange

The exchange of ^{18}O between CO_2 and water catalyzed by carbonic anhydrase in the presence of 4-MI was measured using membrane-inlet mass spectrometry [23]. The reaction solution was in contact with a membrane permeable to gases. CO_2 passing across the membrane entered a mass spectrometer (Extrel EXM-200) providing a continuous measure of isotopic content of CO_2. The uncatalyzed and enzyme catalyzed exchange of ^{18}O between CO_2 and water at chemical equilibrium was measured at 25 °C. The total ionic strength of solution was kept at a minimum of 0.2 M by the addition of Na_2SO_4.

The rates of two processes can be determined from this exchange [23]. R_1 is the rate of interconversion of CO_2 and HCO_3^-, steps that are not dependent on proton transfer. However, we have observed a decrease in R_1 upon increasing concentration of 4-MI, an inhibition of catalysis. These data for R_1 were fitted to Eq. (5). Here, K_I is the equilibrium dissociation constant for 4-MI at a site that is an inhibitor of the binding of substrate. R_1' is the value of R_1 in the absence of 4-MI. The substrate concentration in these experiments is much lower than that of the apparent binding constant of substrate to enzyme; consequently Eq. (5) is consistent with competitive or noncompetitive inhibition

$$R_1 = R_1' K_I/(K_I + [4\text{-MI}]). \quad (5)$$

The second rate, R_{H_2O}, is the proton transfer dependent rate of release from enzyme of $H_2{}^{18}O$ [23]. As demonstrated for catalysis by Zn(II)-H64A HCA II [9,24], imidazole and pyridine derivatives can act as a proton donor to activate catalysis (dehydration direction); the resulting effect on R_{H_2O} is described by Eq. (6). In this equation, R'_{H_2O} is the observed maximal value of R_{H_2O}, and $K_{app}^{4\text{-MI}}$ is an apparent equilibrium dissociation constant of the exogenous activator 4-MI to the enzyme. These data typically showed a very slight inhibition at higher concentrations of 4-MI with inhibition constant K_I. $R^0_{H_2O}$ is the value of R_{H_2O} in the absence of 4-MI

$$R_{H_2O} = R'_{H_2O}\{[4\text{-MI}]/(K_{app}^{4\text{-MI}} + [4\text{-MI}])\} \times \{K_I/([4\text{-MI}] + K_I)\} + R^0_{H_2O}. \quad (6)$$

The constants in Eqs. (5) and (6) were determined by fitting to experimental data using a nonlinear least-squares method (Enzfitter, Elsevier-Biosoft).

Stopped-flow kinetics

Initial rates of CO_2 hydration catalyzed by Co(II)-H64A HCA II were measured at pH 7.8 by following the change in absorbance of a pH indicator, phenol red at 558 nm. Data were taken on an Applied Photophysics (SX.18MV) stopped-flow spectrophotometer. Rates were measured at concentrations of 4-MI ranging from 2 to 100 mM. Total ionic strength was kept at a minimum 0.2 M by addition of Na_2SO_4. CO_2 solutions were prepared by bubbling CO_2 into water at 25 °C with final concentrations after mixing ranging from 0.7 to 17 mM. The initial rates at each concentration of 4-MI were determined from five reaction traces comprising the initial 10% of the reaction. The uncatalyzed rates were determined in a similar manner and subtracted from the total observed rates. Enhancement by the exogenous proton acceptor 4-MI in CO_2 hydration can be described by ping-pong kinetics [2], from which at saturating CO_2 concentrations,

$$k_{cat} = k'_{cat}[4\text{-MI}]/(K_M^{4\text{-MI}} + [4\text{-MI}]). \quad (7)$$

Determination of k_{cat}, k'_{cat}, and $K_M^{4\text{-MI}}$ was carried out by a nonlinear least-squares method.

Visible absorption spectroscopy

The visible absorption spectrum of Co(II)-H64A HCA II, taken on a Hewlett Packard 8453 spectrophotometer, was used to measure the binding of 4-MI to the enzyme. The spectra were measured at 25 °C after addition of increasing amounts of a stock solution of 4-MI (pH 7.9) to a cuvette containing 1 ml of 0.2 mM of Co(II)-H64A HCA II and 0.2 M Na_2SO_4 to control ionic strength. The equilibrium dissociation constant, K_D, of 4-MI was determined by fitting Eq. (8) to the molar absorptivity

$$\varepsilon = (\varepsilon_{max})K_D/(K_D + [4 - MI]). \quad (8)$$

Molecular modeling

The binding of 4-MI to H64A HCA II was simulated on a Silicon Graphics workstation using Sybyl 6.9 (Tripos, Inc.). The initial coordinates for H64A HCA II were taken from a crystal structure which shows two molecules of 4-MI bound in the active-site cavity (Protein Data Bank Accession No. 1MOO [25]). This model was modified to contain one 4-MI molecule (not protonated) with distances between the cobalt and C^2–H, C^5–H, and CH_3 constrained to the values determined from NMR data (Table 1). Charges were estimated using the Gasteiger–Huckel method [26]. A subset minimization process was carried out using the Powell method [27] and a gradient termination, 0.1 kcal/(mol Å).

Results

^1H NMR paramagnetic relaxation

The binding of 4-MI to Co(II)-H64A HCA II was analyzed by measuring the paramagnetic relaxation enhancement, T_{1P}^{-1}, of the proton resonances of 4-MI at 25 °C and pH 7.9. The absence of extensive line broadening for the proton signals of 4-MI and the high values of K_D estimated to be near 200 M (Table 1) suggest that 4-MI is in fast-exchange between the bound and free forms. In fast-exchange, the relaxation rate enhancement can be described by $T_{1P}^{-1} = f_m T_{1M}^{-1}$, where f_m is the mole fraction of bound 4-MI, and the measured relaxation gives averaged distances between bound 4-MI and Co(II) [15]. The relaxation times T_1 for C^2–H, C^5–H, and CH_3 of 4-MI varied from 1.0 to 2.5 s as the concentration of 4-MI was increased; the relaxivities $T_1^{-1}/[E]$ were plotted against 4-MI concentration (Fig. 1). These relaxivities were adequately fit by Eq. (3), consistent with a single binding site for 4-MI within the sphere of influence of the paramagnetic cobalt. Binding constants were in the range of 200–370 mM (Table 1).

A value for the relaxation rate of bound 4-MI, T_{1M}^{-1}, was obtained from Eq. (3) and substituted in the Solomon equation (Eq. 4) to estimate the distance of 4-MI to the cobalt. Since the electronic relaxation time of cobalt in the Co(II)-H64A HCA II system was not measured, a range of electron correlation times τ_c from 5×10^{-13} to 10^{-11} s was studied to obtain distances, assuming that the electron correlation time is predominant in our system. These correlation times depend on the coordination geometry of the metal [21,22]. Substitution into Eq. (4) of the relaxation rate of bound 4-MI, T_{1M}^{-1}, and a long electron correlation time of 10^{-11} s consistent with tetrahedral coordination about the cobalt [21,22] gave distances from 4.9 to 5.8 Å between the protons of 4-MI and the cobalt (Table 1). The distances resulting from substitution into Eq. (4) of a shorter electron correlation time of 5×10^{-13} s consistent with penta-coordination gave distances from 3.5 to 4.1 Å between the protons of 4-MI and the cobalt

Table 1
Proton relaxivity T_{1M}^{-1}, equilibrium dissociation constant K_D, and distance of protons in 4-MI from the cobalt in the interaction of 4-MI with human Co(II)-H64A HCA II[a]

Proton signal	T_{1M}^{-1} (s^{-1})[b]	K_D (mM)[b]	Distance (Å)[c]
C^2–H	360 ± 24	230 ± 50	4.86 ± 0.05
C^5–H	330 ± 70	370 ± 96	4.93 ± 0.18
CH_3	130 ± 23	200 ± 16	5.75 ± 0.17

[a] NMR spectra were taken at 25 °C in solutions at pH 7.9 containing 0.5 mM of Co(II)-H64A HCA II and 8 mM of the reference TSP-d4.
[b] T_M^{-1} and K_D values were obtained by fitting of data to Eq. (3).
[c] Estimated values for the distance between 4-MI and paramagnetic cobalt were calculated using $\tau_c = 10^{-11}$ s in Eq. (4). The distances obtained using $\tau_c = 5 \times 10^{-13}$ s are 3.49 ± 0.04 Å (C^2–H), 3.54 ± 0.13 Å (C^5–H), and 4.13 ± 0.12 Å (CH_3).

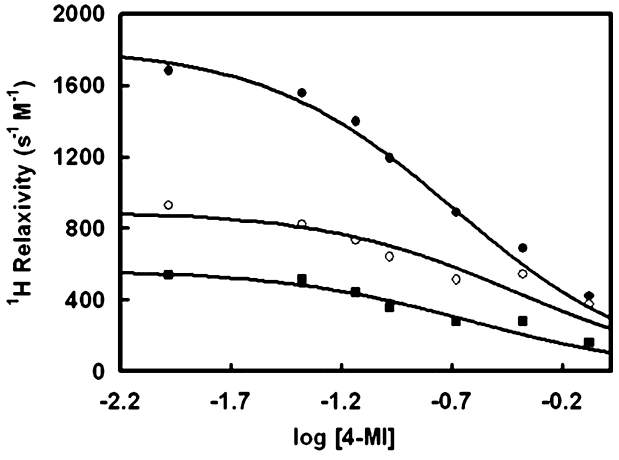

Fig. 1. The dependence on the logarithm of concentration of 4-MI (M) of the proton relaxivities of the C^2-H (●), C^5-H (○), and CH_3 (■) resonances of 4-MI in the presence of 0.5 mM Co(II)-H64A HCA II. The relaxivity is $T_1^{-1}/[E]$ where [E] is total concentration of Co(II)-H64A HCA II. Solutions at pH 7.9 contained no additional buffer. The solid lines are nonlinear least-squares fits of Eq. (3) to the data.

(footnote in Table 1). The electronic absorption spectra discussed below indicate a tetrahedral geometry about the metal in the complex with 4-MI. It is important to emphasize that the distances obtained from these NMR data may represent a weighted average among different binding modes heavily influenced by the $1/r^6$ factor of Eq. (4).

Catalysis

We determined the rate constants in catalysis $R_1/[E]$ and $R_{H_2O}/[E]$ from mass spectrometric measurement of the catalyzed exchange of ^{18}O between CO_2 and water. $R_{H_2O}/[E]$ describes the proton transfer dependent release of ^{18}O-labeled water from the active site (Eq. (6)) and $R_1/[E]$ describes the catalyzed rate of CO_2/HCO_3^- interconversion (Eq. (5)) [23]. Addition of 4-MI caused a weak inhibition of $R_1/[E]$ in catalysis by Co(II)-H64A HCA II (Fig. 2). From these data, an equilibrium dissociation constant K_I of 260 ± 30 mM was estimated using Eq. (5). This value is roughly consistent with the equilibrium dissociation constant from the NMR experiments (200–370 mM).

The values of $R_{H_2O}/[E]$ for Co(II)-H64A HCA II are not significantly enhanced upon addition of 4-MI because bicarbonate itself is a significant proton donor in the exchange of ^{18}O catalyzed by Co(II)-H64A HCA II [28]. However, we show in Fig. 2 the enhancement in $R_{H_2O}/[E]$ for Zn(II)-H64A HCA II upon addition of 4-MI measured by the ^{18}O exchange method (data from Tu et al. [28]). The activation of $R_{H_2O}/[E]$ shown in Fig. 2 can be fit by Eq. (6) with $K_{app}^{4\text{-MI}} = 25 \pm 4$ mM. This binding constant determined by equilibrium ^{18}O exchange represents a tighter binding at a proton transfer site or sites than the binding of 4-MI at the site that causes inhibition of the CO_2 and HCO_3^- interconversion measured by R_1 (Table 2).

We also measured the activation by 4-MI of the CO_2 hydration activity of Co(II)-H64A HCA II under steady-state conditions using stopped-flow spectrophotometry (Fig. 3). Under these initial velocity conditions, the very low concentrations of bicarbonate prevent it from significantly influencing catalysis. We measured the dependence of k_{cat} for CO_2 hydration on concentration of the proton acceptor 4-MI (Eq. (7)) and determined $K_M^{4\text{-MI}}$ to be 17 ± 2 mM (Fig. 3). These data confirm that 4-MI is an activator of catalysis by Co(II)-H64A HCA II. The steady-state constant $K_M^{4\text{-MI}}$ is not a binding constant; however, we note that this value is in the same range as the value $K_{app}^{4\text{-MI}}$ of 25 mM determined for Zn(II)-H64A HCA II by the ^{18}O exchange method. Table 2 compares constants determined by the methods we have used.

The presence of a binding site for 4-MI associated with the side chains of Glu69 and Asp72 detected in a

Table 2
Comparison of constants for the interaction of 4-MI with H64A HCA II

Method	(mM)
Electronic spectra (525 nm) K_D of Eq. (8)	170 ± 30
NMR relaxation (C^2–H) K_D of Eq. (3)	230 ± 50
Inhibition of ^{18}O exchange K_I of Eq. (5)	260 ± 30
Activation of ^{18}O exchange $K_{app}^{4\text{-MI}}$ of Eq. (6)	25 ± 4
Steady-state hydration of CO_2 $K_M^{4\text{-MI}}$ of Eq. (7)	17 ± 2

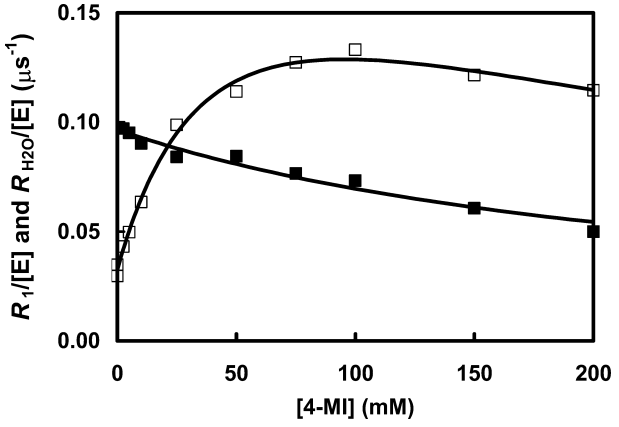

Fig. 2. The dependence on the concentration of 4-MI of (■) $R_1/[E]$ catalyzed by Co(II)-H64A HCA II, and (□) $R_{H_2O}/[E]$ catalyzed by Zn(II)-H64A HCA II. The solid line for $R_1/[E]$ is a least-squares fit of Eq. (5) to the data resulting in $K_I = 260 \pm 30$ mM. The data for $R_{H_2O}/[E]$ are fit by Eq. (6) with $K_{app}^{4\text{-MI}} = 25 \pm 4$ mM. Data were obtained at pH 7.8 and 25 °C with solutions containing 25 mM of all species of CO_2; total ionic strength of solution was maintained at a minimum of 0.2 M by addition of Na_2SO_4.

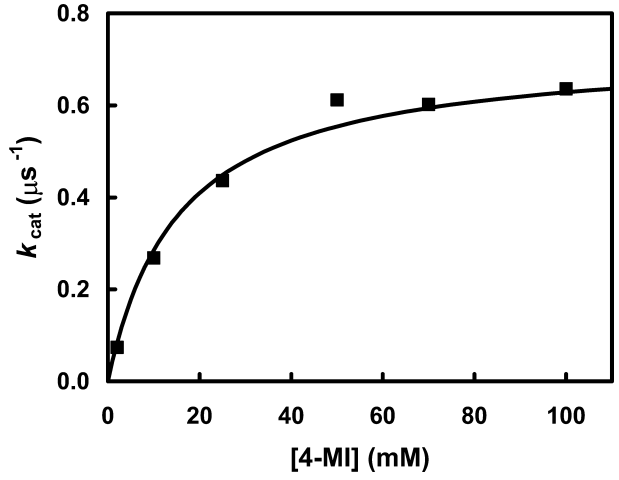

Fig. 3. The dependence on the concentration of 4-MI of k_{cat} for hydration of CO_2 catalyzed by Co(II)-H64A HCA II determined by stopped-flow spectrophotometry. The solid line is a least-squares fit of Eq. (7) to the data resulting in $K_M^{4\text{-MI}} = 17 \pm 2$ mM. Data were obtained at pH 7.8 and 25 °C. Total ionic strength of solution was maintained at a minimum of 0.2 M by addition of Na_2SO_4.

crystal structure of H64A HCA II [25] prompted studies to evaluate whether this binding site was effective in proton transfer. For this purpose, we purified the triple mutant H64A-E69A-D72A HCA II. The addition of 4-methylimidazole at pH 7.8 to this mutant activated $R_{H_2O}/[E]$, the proton transfer dependent release of $H_2{}^{18}O$ (Eq. (6)) from the enzyme (Fig. 4A). This activation appeared to fit a hyperbolic curve; at 200 mM 4-MI there was nearly a fourfold activation of R_{H_2O}. Based on these data, a rough estimate of the binding constant of 4-MI at the proton transfer site or sites on the triple mutant was $K_{app}^{4\text{-MI}}$ of 45 ± 12 mM determined by a fit of Eq. (6) to the data of Fig. 4. This value is compared with that for H64A HCA II of 25 ± 4 mM (Table 2). It was evident from the data on $R_1/[E]$, the rate of interconversion of CO_2 and bicarbonate, that 4-MI caused inhibition of catalysis by both H64A and H64A-E69A-D72A HCA II (Fig. 4B). This presumably is caused by the very weak binding of 4-MI to the zinc. It is interesting that the extent of inhibition appears greater for H64A HCA II than for the triple mutant in Fig. 4. This very weak inhibition was neglected in our estimates of $K_{app}^{4\text{-MI}}$.

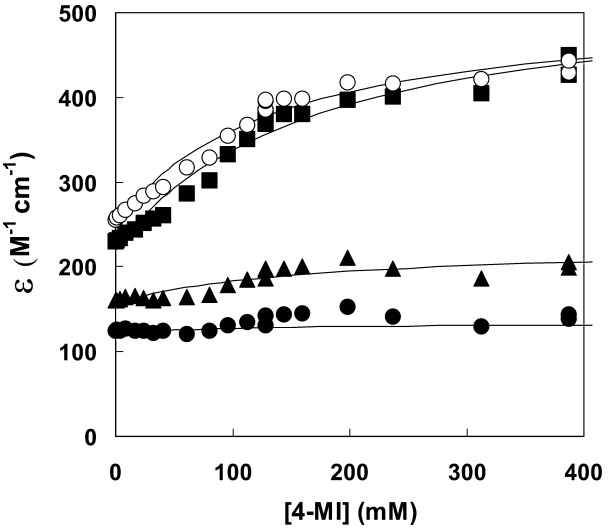

Fig. 5. The molar absorptivities at (■) 525 nm; (○) 560 nm; (▲) 617 nm; and (●) 640 nm as a function of 4-MI concentrations obtained from visible absorption spectra of Co(II)-H64A HCA II at pH 7.8 and 25 °C. Ionic strength was kept at a minimum of 0.2 M by addition of Na_2SO_4. The solid lines are a fit of Eq. (8) to the data resulting in $K_D = 170 \pm 30$ mM from the data at 525 nm, and $K_D = 130 \pm 30$ mM from the data at 560 nm.

Visible absorption spectra

The electronic absorption spectrum of Co(II)-H64A HCA II in the visible region was similar to that of Co(II)-substituted wild-type CA II with peaks at 525, 560, 617, and 640 nm having maximal molar absorptivities of 250–350 $M^{-1}\,cm^{-1}$ at pH near nine [14,29]. There was an increase in absorption as 4-MI was added, especially for the peaks at 525 and 560 nm (Fig. 5). The larger increases in molar absorptivity at 525 and 560 nm were fit with one binding site as described by Eq. (8), both fit by an equilibrium dissociation constant K_D near 170 ± 30 mM for the binding of 4-MI to Co(II)-H64A HCA II (see legend to Fig. 5). This value is consistent with the binding constants determined from the kinetics and NMR experiments (compared in Table 2).

Discussion

The participation of exogenous proton donors and acceptors is necessary to achieve maximal velocity in catalysis by carbonic anhydrase of the hydration of CO_2 and dehydration of HCO_3^- [2,3]. In this aspect, these exogenous proton donors and acceptors are second substrates for carbonic anhydrase. Proton transfer between the zinc-bound water and buffers in solution (Eq. (2)) occurs in steps separate and distinct from the interconversion of CO_2 and HCO_3^- (Eq. (1)). This effect of exogenous proton donors is amplified in the mutant H64A HCA II lacking the internal proton shuttle His64. Proton transfer by 4-MI has been demonstrated by the saturable enhancement of ^{18}O exchange between CO_2 and water catalyzed by H64A HCA II and by

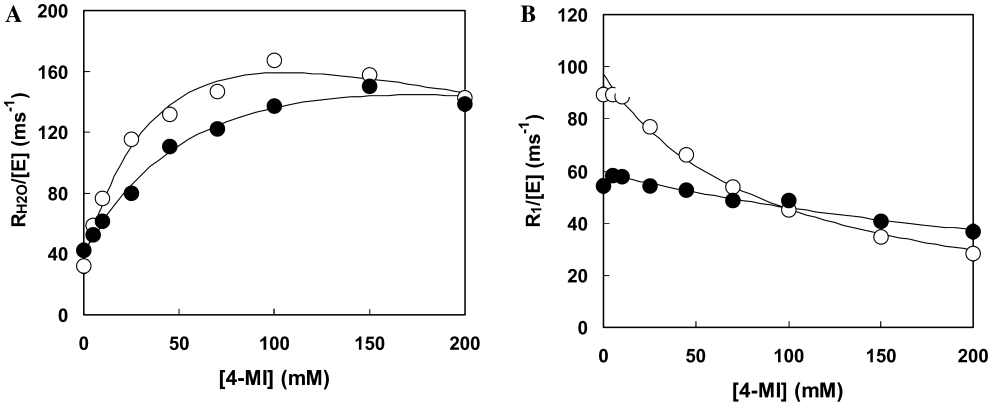

Fig. 4. The effect of 4-MI on (A) $R_{H_2O}/[E]$ and (B) $R_1/[E]$ catalyzed by (○) H64A HCA II, and by (●) H64A-E69A-D72A HCA II. Experimental conditions were as described in Fig. 2.

stopped-flow spectrophotometry [9]. The maximal proton transfer activity of H64A in the presence of saturating levels of 4-MI closely approximates that of wild-type HCA II [10]. This gives significance to the binding sites of 4-MI within the active-site cavity, to learn the location of efficient proton donors and provides an opportunity to comment on the range of distances that are effective in proton transfer in the active site of carbonic anhydrase.

4-MI binding near the metal

We have used Co(II)-H64A HCA II to study the binding properties of 4-MI to the enzyme. The substitution of Zn(II) by Co(II) does not alter the crystal structure of HCA II; the conformation of the Co(II)-substituted enzyme is nearly identical with zinc-containing HCA II, with a root-mean-square deviation for Cα atoms of 0.09 Å [30]. The pK_a near 7 of the catalytic metal-bound water is not altered significantly by this exchange of metals [31]. Moreover, the catalytic activity k_{cat}/K_m for the hydration of CO_2 by the Co(II)-substituted wild-type CA II is similar to the zinc-containing enzyme and represents the metal substitution that retains the highest catalytic activity when compared to nickel, manganese, and others [14,29].

The ^{1}H NMR relaxation of 4-MI caused by Co(II)-H64A HCA II allowed us to estimate the distances of a 4-MI binding site from the cobalt (Table 1). These calculated distances are dependent on the electronic correlation time of the cobalt (Eq. (4)), which is itself dependent on the geometry of coordinating ligands, including 4-MI, to the metal. The equilibrium dissociation constant of 4-MI in complex with Co(II)-H64A HCA II near 200 mM (Table 2) measured by NMR, visible absorption, and inhibition of catalytic activity indicates a binding site of very low affinity. Moreover, the increase in the molar absorbance at 525 and 560 nm to values above 300 $M^{-1}\,cm^{-1}$ upon adding 4-MI (Fig. 5) indicates 4-MI binds closely to the metal though not significantly changing the tetrahedral coordination with His94, 96, and 119, and a solvent molecule as ligands [29,32]. A tetrahedrally coordinated metal in Co(II)-substituted CA is consistent with a long correlation time of $\tau_c = 10^{-11}$ s [21,22]; substitution of this value into Eq. (4) results in distances of 4.9–5.8 Å from C^2-H, C^5-H, and CH_3 of 4-MI to the metal (Table 1). These distances appear similar to other inhibitors of carbonic anhydrase that do not coordinate directly with the metal such as cyanate and nitrate, a mode of binding often found for unprotonated inhibitors that do not donate a hydrogen bond to the Oγ1 of Thr 199 [33]. These inhibitors typically form hydrogen bonds with the backbone NH of Thr 199 and are located in a hydrophobic cavity 3 Å from the metal at the closest. This is the proposed mode of binding of 4-MI to H64A Co(II)-HCA II as determined by NMR. In this binding mode with 4-MI,the cobalt retains a solvent molecule as the fourth ligand in the bound complex, although the geometry about the metal may become distorted tetrahedral.

The distances obtained for a long correlation time $\tau_c = 10^{-11}$ s (Table 1) were used to locate a binding site of 4-MI using a reported crystal structure of (zinc-containing) H64A HCA II (Protein Data Bank Accession No. 1MOO [25]) and assuming that the structure of the cobalt-substituted H64A HCA II is not significantly different. With molecular modeling (Sybyl version 6.9, Tripos, Inc.), we have simulated a binding location of 4-MI. Fig. 6 shows this model with an unprotonated 4-MI molecule positioned at distances constrained to be those given in Table 1. This energy-minimized binding mode shows 4-MI to be oriented face-on to the metal as a second-shell inhibitor. This is in agreement with previous spectroscopic studies showing that 4-MI has no significant binding at the metal in Co(II)-substituted bovine carbonic anhydrase II [34]. The binding of 4-MI in Fig. 6 appears to be stabilized by interaction of the N1 of 4-MI with the NH of Thr 199 at 3.3 Å. This distance is too long for a significant hydrogen bond; however, the calculation is certainly affected by the uncertainties in the distances of Table 1, and these simulations suggest that such a hydrogen bond is formed in the inhibited complex. In addition, the methyl group of 4-MI forms hydrophobic interactions with the side chains of residues Val 121 and Val 143 on the hydrophobic side of the active-site cavity. In this configuration, 4-MI displaces the "deep water" in the hydrophobic cavity formed by residues 121 and 143 that have often been suggested as the catalytic binding site of CO_2 [3].

The binding constant of 4-MI near 200 mM determined by spectroscopic methods and inhibition of catalysis (Table 2) can be contrasted with the value of the apparent equilibrium dissociation constant $K_{app}^{4\text{-MI}}$ of 25 ± 4 mM (Eq. (6)) for 4-MI in the activation of catalysis by H64A HCA II (Fig. 2). This value was determined by ^{18}O exchange at chemical equilibrium, and although not strictly an equilibrium binding constant it represents a value that we estimate is close to the true binding constant at the productive binding sites for 4-MI. Strictly, $K_{app}^{4\text{-MI}}$ of Eq. (6) includes the binding of substrate 4-MI in all enzyme species that contribute to the proton transfer steps of catalysis [35]. These data demonstrate that the binding site near the metal of 4-MI as estimated by NMR (Fig. 6) is inhibitory and is not a site from which there is significant contribution of proton transfer in catalysis.

Other 4-MI binding sites

Two other different binding sites for 4-MI in the active site of H64A HCA II were found by crystallography and reported previously; one forms a π stacking interaction with the indole side chain of Trp5 [9,10]. A second

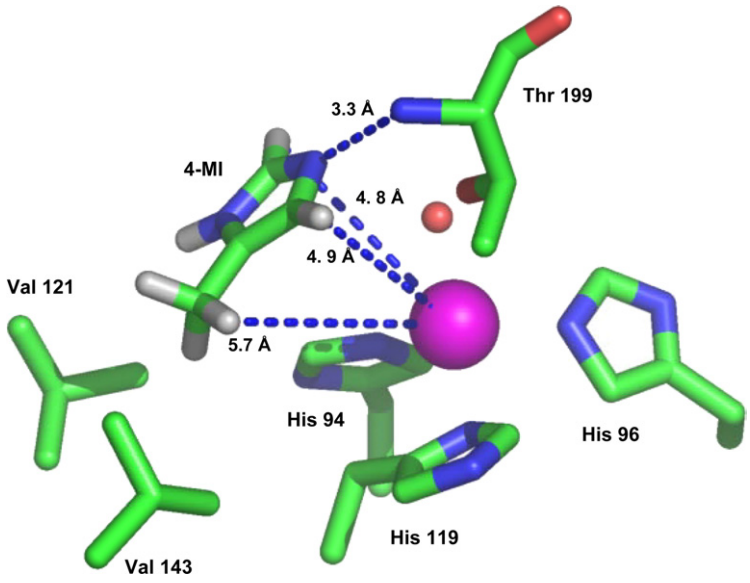

Fig. 6. The active site of H64A HCA II showing a binding position of 4-MI consistent with the NMR data. The cobalt ion (purple sphere) is coordinated to His 94, 96, and 119, and to a cobalt-bound solvent molecule (orange sphere). 4-MI is shown in an energy minimized (Sybyl 6.9) location with distances constrained to those determined by NMR (Table 1). Also shown are the backbone NH of Thr 199 close to the N1 of 4-MI, and hydrophobic residues Val 143 and Val 121 near the methyl group of 4-MI. (For interpretation of the references to color in this figure legend, the reader is referred to the web version of this paper.)

is situated adjacent to the side chains of Glu69 and Asp72 [25], near a binding site for histamine in the active-site cavity of HCA II [11]. 4-MI binding at both of these sites participates in hydrogen bonding with ordered water in the active-site cavity; however, a completed proton transfer pathway from these binding sites of 4-MI to the zinc-bound water cannot be observed from the crystal structures [9,25]. Nevertheless, 4-MI as a proton donor activated the catalysis of ^{18}O exchange catalyzed by both H64A and W5A-H64A HCA II [9], and by H64A and H64A-E69A-D72A HCA II (Fig. 4), with nearly superimposable kinetics showing that these binding sites for 4-MI are nonproductive in catalysis of the hydration of CO_2.

These experiments, along with previously reported crystallographic and catalytic data given in Table 3, present an array of distances of potential proton donors to the metal in carbonic anhydrase II (and one example of CA V). These considerations help establish distances for significant proton transfer in the active-site cavity of carbonic anhydrase. The binding site of 4-MI about 4.5 Å from the metal determined in this NMR study is so close to the metal as to be inhibitory to catalysis, and perhaps too near the metal to transfer protons between the metal-bound solvent and solution. The binding sites for 4-MI found by crystallography at 12–13 Å are too distant from the metal-bound solvent to transfer protons.

The significance of the distance between the donor and acceptor in proton transfer in catalysis by carbonic anhydrase is usually discussed in terms of the number of intervening water molecules since many calculations

Table 3
Rate constants for proton transfer and approximate distances between proton donor and zinc in catalysis by carbonic anhydrase

Enzyme	Proton donor	Distance to zinc (Å)	$k_{\text{proton transfer}}$ (ms^{-1})
Co(II)-H64A CA II	4-MI	4.5	Inhibitory
H64A-T200H CA II[a]	His200	5.5	300
H64A-N67H CA II[b]	His67	6.6	200
Wild-type CA II	His64	7.5	800
H64A-N62H CA II[b]	His62	8.2	30
Y131C CA V[c]	Modifying imidazole	8.4	3
H64A CA II[d]	4-MI (Trp5 site)	12	Not detected
H64A CA II[e]	4-MI (Glu69, Asp72 site)	13	Not detected

[a] D. Bhatt, Z. Fisher, C.K. Tu, R. McKenna, D.N. Silverman, unpublished.
[b] Ref. [8].
[c] Ref. [39].
[d] Ref. [9,10].
[e] Ref. [25].

have shown that the barrier height for proton transfer depends on the solvent structure in the active site. Cui and Karplus [36] have presented density functional calculations of proton transfer through intervening hydrogen-bonded water in modeled active sites of carbonic anhydrase. The calculated barrier height for proton transfer was seen to increase with the number of intervening water molecules. In addition, calculations show that the barrier height should include the energy needed to organize the water bridge in the active site, up to 2–3 kcal/mol as calculated by Lu and Voth [37]. Further calculations also emphasize the effect of peripheral water molecules, not directly in the proton transfer pathway, to increase the barrier height [37,38].

The location of efficient proton donors is near 7 Å from the metal: His64 in HCA II (7.5 Å from the zinc); and His67 in H64A-N67H HCA II (6.6 Å) (Table 3). Of course, there are considerations other than distance which influence proton transfer rates in carbonic anhydrase, for example, the effect of nearby residues on the range of side-chain conformations of the proton donor [39,40] and water structure in the active site [41]. Nevertheless, the data of Table 3 establish that distance is a prominent consideration and show the range of distances in the active site of HCA II for which proton transfer is efficient.

Acknowledgments

We are pleased to acknowledge the assistance of James R. Rocca and the National High Magnetic Field Laboratory at the University of Florida in the NMR paramagnetic relaxation experiments. We thank the Advanced Magnetic Resonance Imaging and Spectroscopy (AMRIS) facility in the McKnight Brain Institute (University of Florida) where the NMR studies were performed. We thank Zoë Fisher for help with structural aspects of this work. This work was supported by grants from the Maren Foundation (I.E.) and the NIH GM 25154 (D.N.S.).

References

[1] D. Hewett-Emmett, R.E. Tashian, Mol. Phylogenet. Evol. 5 (1996) 50–77.
[2] S. Lindskog, Pharmacol. Ther. 74 (1997) 1–20.
[3] D.W. Christianson, C.A. Fierke, Acc. Chem. Res. 29 (1996) 331–339.
[4] H. Steiner, B.-H. Jonsson, S. Lindskog, Eur. J. Biochem. 59 (1975) 253–259.
[5] C.K. Tu, D.N. Silverman, C. Forsman, B.-H. Jonsson, S. Lindskog, Biochemistry 28 (1989) 7913–7918.
[6] A.E. Eriksson, T.A. Jones, A. Liljas, Proteins 4 (1988) 274–282.
[7] S.K. Nair, D.W. Christianson, J. Am. Chem. Soc. 113 (1991) 9455–9458.
[8] S.Z. Fisher, J. Hernandez, C.K. Tu, D. Duda, C. Yoshioka, H. An, L. Govindasamy, D.N. Silverman, R. McKenna, Biochemistry 44 (2005) 1097–1105.
[9] H. An, C.K. Tu, D. Duda, I. Montanez-Clemente, K. Math, P.J. Laipis, R. McKenna, D.N. Silverman, Biochemistry 41 (2002) 3235–3242.
[10] D. Duda, C.K. Tu, M.Z. Qian, P.J. Laipis, M. Agbandje-McKenna, D.N. Silverman, R. McKenna, Biochemistry 40 (2001) 1741–1748.
[11] F. Briganti, S. Mangani, P. Orioli, A. Scozzafava, G. Vernaglione, C.T. Supuran, Biochemistry 36 (1997) 10384–10392.
[12] F.W. Studier, A.H. Rosenberg, J.J. Dunn, J.W. Dubendorf, Methods Enzymol. 185 (1990) 60–89.
[13] R.G. Khalifah, D.J. Strader, S.H. Bryant, S.M. Gibson, Biochemistry 16 (1977) 2241–2247.
[14] S. Lindskog, B.G. Malmstrom, J. Biol. Chem. 237 (1962) 1129–1137.
[15] I. Bertini, C. Luchinat, NMR of Paramagnetic Molecules in Biological Systems, Benjamin/Cummings, Menlo Park, CA, 1986.
[16] S. Poli-Scaife, R. Attias, P.M. Dansette, D. Mansuy, Biochemistry 36 (1997) 12672–12682.
[17] M.N. Harris, C.M. Bertolucci, L.-J. Ming, Inorg. Chem. 41 (2002) 5582–5588.
[18] I. Solomon, Phys. Rev. 99 (1955) 559–565.
[19] I. Solomon, N. Bloembergen, J. Chem. Phys. 25 (1956) 261–266.
[20] S. Koenig, R.D. Brown, I. Bertini, C. Luchinat, Biophys. J. 41 (1983) 179–187.
[21] I. Bertini, C. Luchinat, A. Rosato, Prog. Biophys. Mol. Biol. 66 (1996) 43–80.
[22] I. Bertini, C. Luchinat, S. Aime, Coord. Chem. Rev. 150 (1996) 77–110.
[23] D.N. Silverman, Methods Enzymol. 87 (1982) 732–752.
[24] S. Taoka, C.K. Tu, K.A. Kistler, D.N. Silverman, J. Biol. Chem. 269 (1994) 17988–17992.
[25] D. Duda, L. Govindasamy, M. Agbandje-McKenna, C.K. Tu, D.N. Silverman, R. McKenna, Acta Crystallogr. D 59 (2003) 93–104.
[26] J. Gasteiger, M. Marsili, Tetrahedron Lett. 34 (1978) 3181–3184.
[27] M.J.D. Powell, Comput. J. 7 (1964) 155–162.
[28] C.K. Tu, B.C. Tripp, J.G. Ferry, D.N. Silverman, J. Am. Chem. Soc. 123 (2001) 5861–5866.
[29] I. Bertini, C. Luchinat, A. Scozzafava, Struct. Bonding 48 (1982) 45–92.
[30] K. Håkansson, A. Wehnert, J. Mol. Biol. 228 (1992) 1212–1218.
[31] S. Lindskog, Biochemistry 5 (1966) 2641–2646.
[32] I. Bertini, G. Canti, C. Luchinat, A. Scozzafava, J. Am. Chem. Soc. 100 (1978) 4873–4877.
[33] A. Liljas, K. Håkansson, B.-H. Jonsson, Y. Xue, Eur. J. Biochem. 219 (1994) 1–10.
[34] G. Alberti, I. Bertini, C. Luchinat, A. Scozzafava, Biochim. Biophys. Acta 668 (1981) 16–26.
[35] I. Simonsson, B.-H. Jonsson, S. Lindskog, Eur. J. Biochem. 93 (1979) 409–417.
[36] Q. Cui, M. Karplus, J. Am. Chem. Soc. 124 (2002) 3093–3124.
[37] D. Lu, G.A. Voth, J. Am. Chem. Soc. 120 (1998) 4006–4014.
[38] A. Isaev, S. Scheiner, J. Phys. Chem. B 105 (2001) 6420–6426.
[39] K.M. Jude, S.K. Wright, C.K. Tu, D.N. Silverman, R.E. Viola, D.W. Christianson, Biochemistry 41 (2002) 2485–2491.
[40] R.W. Heck, P.A. Boriack-Sjodin, M.Z. Qian, C.K. Tu, D.W. Christianson, P.J. Laipis, D.N. Silverman, Biochemistry 35 (1996) 11605–11611.
[41] J.E. Jackman, K.E. Merz, C.A. Fierke, Biochemistry 35 (1996) 16421–16428.